

Thermal condensations in hydrostatic coronal loops*

*César A. Mendoza-Briceño***

*Centro de Astrofísica Teórica (CAT), Facultad de Ciencias,
Universidad de los Andes, Mérida, Venezuela.*

Recibido: 13-02-06 Aceptado: 13-12-06

Abstract

The equations of thermal equilibrium along a symmetric coronal loop with a constant cross-sectional area including gravity is investigated. A coronal heating function depending on distance along the loop is considered. The effects of varying the values of the parameters involved in the governing equations are also analyzed. It is found that there is a critical decay length of the heating, below which a hot coronal loop does not exist. It is suggested that thermal non-equilibrium occurs, allowing for the existence of catastrophic cooling. In addition, it is shown that prominence-type equilibria are possible. A distortion of the magnetic field simulating a dip is also studied.

Key words: Coronal heating; coronal loops; hydrodynamics; prominences; Sun.

Condensaciones térmicas en lazos coronales hidrotáticos

Resumen

Las ecuaciones del equilibrio térmico a lo largo de un lazo coronal simétrico con sección transversal constante incluyendo gravedad se investigan. Una función de calentamiento coronal dependiendo de la distancia a lo largo del lazo es considerado. Los efectos de variar los valores de los parámetros implicados en las ecuaciones que gobiernan también se analizan. Se encuentra que hay una longitud crítica del decaimiento del calentamiento por debajo de la cual un lazo coronal caliente no existe. Se sugiere que ocurre un desequilibrio térmico, permitiendo la existencia de un enfriamiento catastrófico. Además, se muestra que los equilibrios tipo prominencia son posibles. Una deformación del campo magnético que simula una depresión del mismo también se estudia.

Palabras clave: Calentamiento coronal; hidrodinámica; lazos coronales; prominencias; sol.

1. Introduction

The solar corona is entirely structured by the solar magnetic field, mostly into loop-like closed flux tubes. It is believed that

these features are the building blocks of the solar corona and their emission dominates the X-ray coronal luminosity. In order to account for the observations, the thermal

* Trabajo presentado en el I Congreso Venezolano de Física, Facultad de Ciencias, Universidad de Los Andes, Mérida, 1997.

** Autor para la correspondencia. E-mail: cesar@ula.ve

structure of coronal loops, have been modelled by several authors. The key assumptions in these models are that the plasma beta (defined as the ratio of the plasma pressure to the magnetic pressure) is small in the corona so that a one-dimensional approximation can be used in which the magnetic field acts only to define a rigid tube geometry, and that the loop heating varies on a time scale long compared to radiative cooling so that static approximation can be used. For instance, Rosner *et al.* (1), Hood and Priest (2), Craig *et al.* (3), Hood and Anzer (4), Steele and Priest (5), have investigated loops for which solar gravity can be neglected. In this category Hood and Anzer (4), Steele and Priest (6) included the effect of cross-section area variation. Steele and Priest (7, 8) included the consideration of a coronal arcade rather than simple loop. Recently, Mendoza-Briceño and Hood (9) studied the effect of spatially dependent heating on the thermal equilibrium of coronal loops.

The effect of solar gravity was included by Vesecky *et al.* (10), Wragg and Priest (11), Serio *et al.* (12), She *et al.* (13), Hood and Anzer (4), Steele and Priest (14) and Mendoza-Briceño (15).

In the present paper the temperature structure along a coronal magnetic loop is studied in the presence of gravity as well as a magnetic dip. The cross-sectional area is considered constant and a heating function which decays with altitude is assumed. Since one of the motivations in this paper is to model prominences, great emphasis will be put on finding those solutions which give hot-cool loops.

2. Equations of Thermal Equilibrium

For static, steady coronal loops, the variation of dimensionless temperature T (normalised to 10^5 K) and dimensionless pressure (p) along a coronal loop obey the equations for hydrostatic equilibrium and the energy equation i.e.

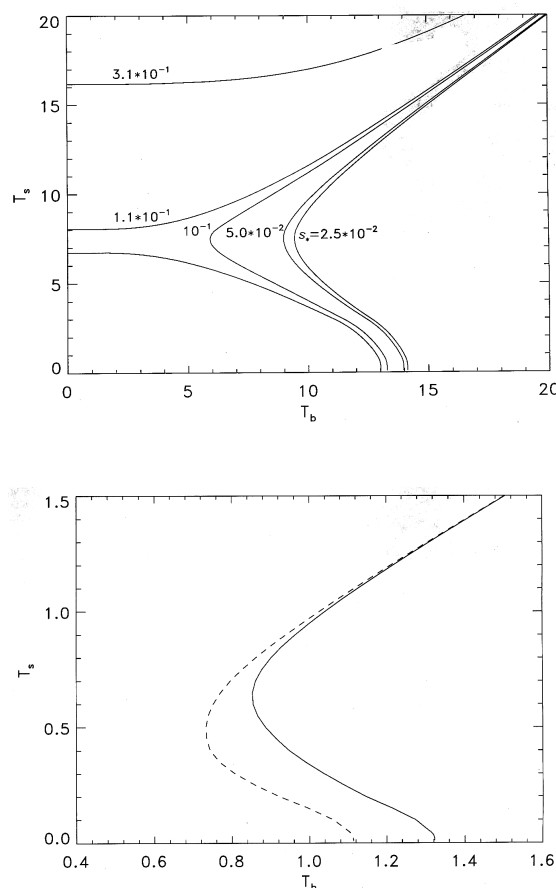


Figure 1. The summit temperature T_s as a function of the boundary temperature T_b (a) for different values of the decay length of the heating s_0 . Parameters used are $L_* = 1248.0$ and $h_* = 3.96 \times 10^{-2}$, (b) for the case gravity without dip (dashed line) and with dip (solid line).

$$\frac{dp}{ds} = \frac{P}{T} g(s) \quad [1]$$

$$\frac{d}{ds} \left(T^{\frac{5}{2}} \frac{dT}{ds} \right) = L_*^2 \left[p^2 \chi T^{\alpha-2} - h_* \exp\left(-\frac{1-s}{s_*}\right) \right] \quad [2]$$

with boundary conditions,

$$\frac{dT}{ds} = 0 \text{ at } s = 0 \text{ summit,}$$

$$T = T_b \quad p = p_b \text{ at } s = 1 \text{ footpoint} \quad [3]$$

where s represents the position in the loop, and χ and α are radiative loss coefficient Hildner (16). These equations are governed by three dimensionless parameters, namely L_* proportional to the loop length, h_* is the base heating and s_* is the decay length of the heating. $g(s)$ is the component of solar gravity along the magnetic field which has two components, one describing the general semicircular shape of the field and the other one a dip representing the distortion of the magnetic field

$$g(s) = \frac{1}{1+g_1} \frac{L_0}{\Lambda} \left(\sin \frac{\pi}{2} s - g_1 \frac{3\pi}{2} s \right)$$

where L_0 is the half-length of the loop, Λ is the gravitational scale-length, and g_1 is the amplitude of the distortion which is taken in paper as $g_1 = 0.5$ Mendoza-Briceño (15).

The obvious consequence when gravity is included is that the pressure is no longer constant and that it must decrease along the loop from footpoint to summit.

3. Numerical Results

3.1. Hydrostatic Thermal Equilibrium without a Magnetic Dip

When the effect of the magnetic distortion is neglected $g_1 = 0$, Figure 1a shows the summit temperature as a function of boundary temperature, for fixed values of $L_* = 1248.01$, $h_* = 3.96 \times 10^2$. These parameters correspond to a loop length of 4×10^7 m and a heating at the base of 10^{-4} Wm^{-3} . The different curves are labelled with the corresponding value of s_* . Every point in the curve of this figure corresponds to a static solution, whereas every curve is a family of solutions.

When one considers the case where a particular boundary condition is taken, for example $T_b = 5$, solutions at equilibrium ex-

ist only when $s_* \leq s_c (= 1.05 \times 10^{-1})$. From this value upwards there are two-valued solutions where summit temperature increases in the upper branch while it decreases in the lower branch. If the value of s_* is increased, there is a value at which a hot solution exists. Very high values of s_* would correspond to a uniform heating, as expected.

The parameter s_* is the heating deposition scale height. When s_* is decreased the heating along the loop is more concentrated at the base of the loop. The input of energy at the summit is then reduced and the energy balance should be established by the thermal conduction. If less energy is supplied into the structure, then the summit temperature of the structure is lowered.

Decreasing even further the value of s_* , a critical value is reached and the thermal conduction becomes unable to balance the energy losing and hot solution does not exist, as far as the static condition is concerned. However, if dynamics is taken into account the structure should evolve to a new equilibrium with a cooler summit Mendoza and Hood (17).

3.2. Hydrostatic Thermal Equilibrium with a Magnetic Dip

The thermal balance of loops has been studied by assuming that the magnetic configuration of the loop is specified through the function $g(s)$ which is the component of the gravity along the field line. This function $g(s)$ for a semicircular loop has already been investigated in the previous section. In this section, we are interested in focussing our attention on the effect of a dip on the magnetic configuration, which is of great importance for supporting prominences material (Kippenhahn and Schlüter (18); Kuperus and Raadu (19)). A number of models of prominence formation showing the additional effect of the dip have been presented by several authors (Poland and Mariska (20); Mok *et al.* (21); Antiochos and Klimchuk (22); Van Hoven *et al.* (23)).

Poland and Mariska (20) constructed the initial equilibrium with a gravitational potential well at the midpoint whereas other authors viz., Mok *et al.* (21) and Van Hoven *et al.* (23) added the distortion of the projected gravitational force as the condensation forms. In particular, it was added when a substantial condensation (with density > 5 times the nearby coronal value) formed. Mok *et al.* (21) also found prominence formation without dip and argued that it was not clear in Poland and Mariska 's case whether the reversed gravity is essential to draw the plasma to the centre during the condensation process.

In this section the hydrostatic model is employed and the effect of a dip on the magnetic configuration is studied.

The summit temperature as a function of boundary temperature is shown in Figure 1b. This figure shows the effect of the dip; if one locates at the turning point then it is shifted to the right when the dip is included. This effect is very interesting because for fixed values of the parameters the effect of the inclusion of the dip is to reduce the existence of thermal equilibrium.

The pressure and temperature profiles have been plotted in Figure 2 for different values of s . In this case only the hot solution for those values of s , have been drawn. In Figure 2a, the temperature profile shows that the summit temperature decreases when s , decreases, however, for $s, > 0.147$ thermal equilibrium is no longer found. The temperature also decreases when s , decreases in Figure 2b, but the value of s , at which there is no thermal equilibrium is at $s, > 0.16$. As can be seen in this figure, the effect of including a dip is to shift the critical decay length of the heating for the appearance of non-equilibrium to higher values. It is seen from this result that a coronal loop under particular conditions namely, fixed values of L , s , and h , could suffer a catastrophic cooling when a dip starts to form.

3.3. Hot-Cool Solutions

Gravitational effects were considered by Hood and Anzer (4) and Steele and Priest (14). Nonetheless, hot-cool solutions were not found. Steele and Priest (14) by considering a small value of gravity, found several solutions, but hot-cool solutions were difficult to find and were only possible for unrealistic values of gravity. More recently, van den Oord and Zuccarello (24) arrived at the same conclusion that for loops in hydrostatic equilibrium a hot-cool solution cannot be found. However, when the heating function has a spatial dependence, as considered in this paper, cool condensations (hot-cool solutions) can be obtained. First of all, assuming that the typical prominence values are known from observations, then the integration is started from the summit to the footpoint. Secondly, the values of the parameters L , and h , were fixed, and an iteration of the parameter s , was performed.

Figure 3 is a plot of temperature as a function of s for the values of the parameter L , h , and s , given in Table 1. In this figure, prominence-like solutions are shown where the cool summit is at $T_s = 0.2$ (in units of $10^5 K$) and a hot coronal part can be seen between the summit and the footpoint. Here the footpoint temperature is at a chromospheric value.

In Figure 3, the temperature profiles show a maximum of temperature close to $s = 1$ (footpoint) which is shifted to the right when L , is increased. This shift occurs as a result of the decay length decreasing to satisfy the boundary conditions.

Figure 4 shows the pressure profiles for the temperatures shown in Figure 3. As seen the pressure increases from the summit to the footpoint. The four curves start from $p = 1$ at the summit due to the fact that the integration starts from known prominence pressures and temperatures. Here, one sees that the pressure at the footpoint increases when L , increases.

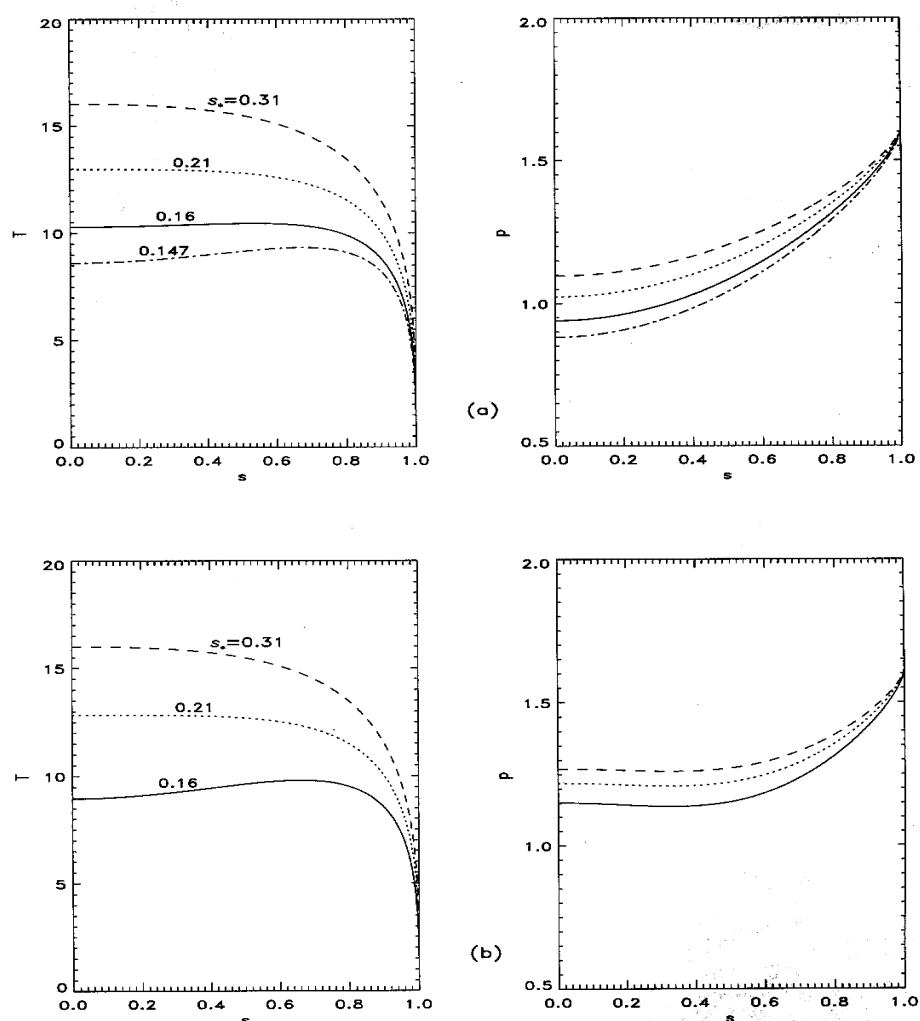


Figure 2. Temperature and pressure profiles for different values of the decay length of the heating s , for a) no dip and b) with a dip.

Table 1
Parameters obtained for prominences solution

	L	S	h	T_{\max}
1	936.01	3.76×10^2	$3.96 \times 10E^{-2}$	11.01
2	1247.01	3.09×10^2	$3.96 \times 10E^{-2}$	12.33
3	1560.01	2.71×10^{-1}	$3.96 \times 10E^{-2}$	13.50
	1872.02	2.44×10^{-1}	$3.96 \times 10E^{-2}$	14.36
4	1968.43	2.37×10^{-1}	$3.96 \times 10E^{-2}$	14.80

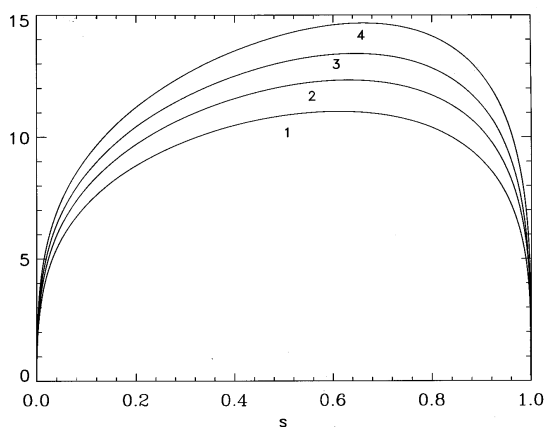


Figure 3. The variation of temperature along a loop from the summit at $s = 0$ to the footpoint at $s = 1$. The numbers refer to the listed values given in Table 1.

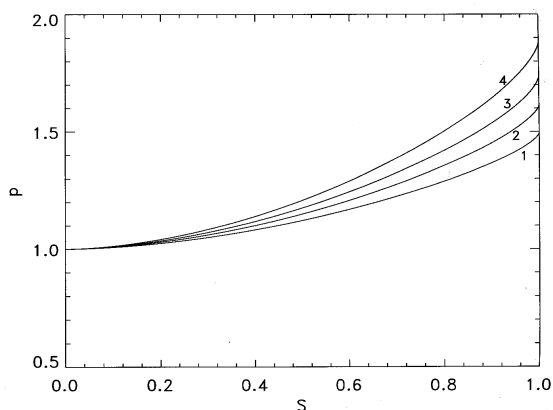


Figure 4. The variation of pressure along a loop from the summit at $s = 0$ to the footpoint at $s = 1$. The numbers refer to the listed values given in Table 1.

In Figure 5 $T^{6/2}dT/ds$ is plotted as a function of T . This is the phase plane diagram for the same solutions as in Figure 3. The flux increases when L , increases. Now, it is interesting to note how the contours from the footpoint (which start at non-zero negative value of $T^{6/2}dT/ds$) to the summit where $T^{6/2}dT/ds = 0$ are closed contours. This is the

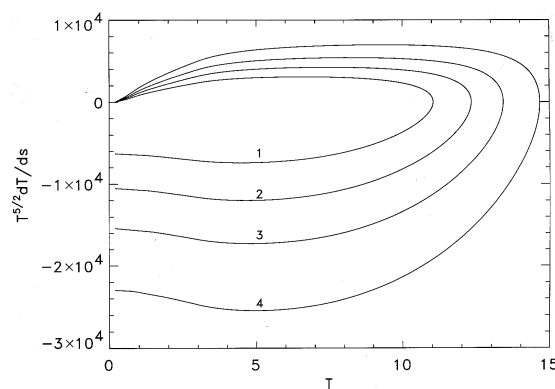


Figure 5. The phase plane diagram for the solutions given in Figure 3.

characteristic behaviour of non-autonomous systems.

4. Summary and Conclusions

The present paper has modelled a coronal loop by a single field line, along which the plasma is in both thermal and hydrostatic equilibria.

Gravity in the hydrostatic equation was considered to have two parts, (i) one part assuming that the loop has a semicircular shape and (ii) the other part simulating a distortion of the loop summit due to a dip in the magnetic field.

In Section 3.2 the effect of a dip was studied. It was found that the pressure first decays and then increases along the loop starting from the footpoint. The effect of a dip is to increase the summit pressure, which increases the radiation (the heating does not change) and so reduces the summit temperature below the value for gravity without a dip.

It was observed, that the lack of equilibrium Hood and Priest (2); Roberts and Frankenthal (25) can occur when decay length of the heating is decreased. However, the critical value of s , is higher when the dip is considered.

In contrast with other authors e.g. Steele and Priest (14), prominence-like solutions were found in this study. The difference between their work with the present study is in the form of the heating function. The heating function considered here has a spatial dependence. The inclusion of gravity as can be seen by using a phase diagram Hood and Anzer, (4); Steele and Priest (14) produces a open contour when a heating does not have a spatial dependence, but when it is considered with spatial variation in which it decays along the loop from the summit produces a closed contour as it was shown in Figure 5.

In conclusion, this paper has therefore, shown that hot and hot-cool loop (prominence-like solution) are possible in hydrostatic equilibrium when heating function is considered to decay with altitude.

References

1. ROSNER R., TUCKER W.H., VAIANA G.S. *Astrophys J.* 220: 643-665, 1978.
2. HOOD A.W., PRIEST E.R. *Astron Astrophys* 77: 233-251, 1979.
3. CRAIG I.L., McCLYMONT A.N., UNDERWOOD J.H. *Astron Astrophys* 70: 1-11, 1978
4. HOOD AW., ANZER, V. *Solar Phys* 115: 61-68, 1988.
5. STEELE C.D.C., PRIEST E.R. *Solar Phys* 125: 295-319, 1990a.
6. STEELE C.D.C., PRIEST E.R. *Solar Phys* 132: 293-306, 1991a.
7. STEELE C.D.C., PRIEST E.R. *Solar Phys* 127: 65-94, 1990b.
8. STEELE C.D.C., PRIEST E.R. *Solar Phys* 134: 73-95, 1991b.
9. MENDOZA-BRICEÑO C.A., HOOD A.W. *Astron Astrophys* 325: 791-802, 1997.
10. VESECKY J.F., ANTIOCHOS S.K., UNDERWOOD J.H. *Astrophys J* 233: 987-997, 1979.
11. WRAGG M.A., PRIEST E.R. *Solar Phys* 70: 293-313, 1981.
12. SERIO S., PERES G., VAIANA G.S., GOLUB L., ROSNER R. *Astrophys J* 243: 288-300, 1981.
13. SHE Z.S., MALHERBE J.M., RAADU M.A. *Astron Astrophys* 164: 364-372, 1986
14. STEELE C.D.C., PRIEST E.R. *Astron Astrophys* 292: 291-303, 1994.
15. MENDOZA-BRICEÑO C.A. The nonlinear thermal evolution of coronal structures, (Ph. D. Thesis), University of St. Andrews, St. Andrews, Scotland, pp. 140, 1996.
16. HILDNER E. *Solar Phys* 35: 123-136, 1974.
17. MENDOZA C.A., HOOD, A.W. *Astrophysical Letters and Communications* 34: 107-112, 1996.
18. KIPPENHAHN R., SCHLÜTER A. *Zs Ap* 43: 36-62, 1957.
19. KUPERUS M., RAADU M.A. *Astron Astrophys* 31: 189-193, 1974.
20. POLAND A.I., MARISKA J.T. *Solar Phys* 104: 303-312, 1986.
21. MOK DRAKE, J.F., SCHNACK D.D., VAN HOVEN, G. *Astrophys J* 359: 288-231, 1990.
22. ANTIOCHOS S.K., KLIMCHUK, J.A. *Astrophys J* 378: 372-377, 1991.
23. VAN HOVEN G., MOKY., DRAKE, J.F. *Solar Physics* 140: 269-287, 1992.
24. VAN DEN OORD G.H.J., ZUCCARELLO F. *Proceedings of IAUSymp.* Stellar Surface STRUCTURE, Ed. K.G. STRASSMEIER. pp. 76, 1996.
25. ROBERTS B., FRANKENTHAL S. *Solar Phys* 68: 103-109, 1980.